# Three dimensional arbitrary voxel shapes in spectroscopy with sub-millisecond echo times

Jeff Snyder[1], Martin Haas[1], Iulius Dragonu[1], Juergen Hennig[1], and Maxim Zaitsev[1]
[1]*Dept. of Radiology, Medical Physics, University Medical Center Freiburg, Freiburg, Germany*

## Introduction

The two most common magnetic resonance spectroscopy (MRS) single-voxel applications, PRESS and STEAM, rely on three gradient and radiofrequency pulse pairs to excite three planes or slices in the sample. Only the region of intersection of the slices produces the fully refocused signal available for detection. These inherent restrictions in slice-selective excitation schemes dictate parallelepiped voxel geometry and lengthen the duration of the excitation module. Therefore, conformation of the voxel to anatomical and pathological targets is problematic resulting in partial-volume effects. Additionally, valuable short-echo time information is lost. In this study, we propose a single 3D spatial and spectral excitation pulse strategy, which allows the definition of 3D arbitrarily-shaped voxels and the possibility of acquisition immediately following excitation, with transverse decay times in the microsecond range. The method is demonstrated in vivo on a clinical 3 T scanner.

## Methods

Spatial selectivity was achieved by a 3D RF-weighted excitation k-space trajectory consisting of 8 concentric spheres or shells each with 8 surface paths spiraling along the surface from the north to south poles (Fig. 1). The target pattern (a 3D curved corkscrew shape, see Fig. 2) was interpolated over a 16x16x16 point grid in excitation k-space, resulting in 4096 points required for full sampling. The entire pulse length for the complete 64 paths was 51.8 ms, requiring segmentation for broad bandwidth spectroscopy applications. Therefore, the trajectory was divided into 64 segments (1,2) using a spatial domain algorithm (3) – each corresponding to an individual surface path – resulting in complete target excitation following 64 acquisitions. The spectroscopy sequence used was a modified pulse-acquire type, with acquisition immediately following the 3D selective pulse. This allowed signal acquisition less than 1 ms (935 µs) following the start of the segment with individual RF pulse lengths of 810 µs (51.8 ms / 64 segments), and including allocation for gradient ramps and coil lead times. Other sequence parameters included a TR of 1500 ms and 128 averages corresponding to 2 acquisitions of each segment. To qualitatively visualize the spatial localization of the pulses, a 3D gradient echo sequence was used with TE/TR = 3/8 ms, an in-plane resolution of 128x128 and 20 axial encoding steps of 10 mm thickness. The pulse amplitudes were scaled down to 10% to mitigate T1 saturation effects. In vivo measurements were performed on healthy human volunteers giving informed consent using a Siemens 3 T Magnetom Trio system (Erlangen, Germany). The 3D localization with similar sequence parameters was also implemented in homogeneous cylindrical phantom experiments to illustrate the excitation target shape. Spectral analysis was performed by LCModel (4).

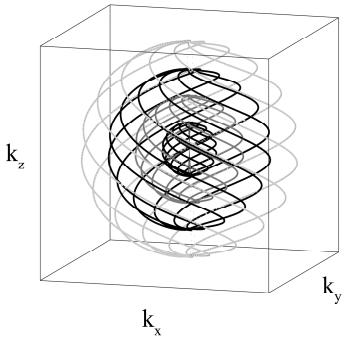


*Figure 1: Trajectory design for 3D selective excitation. Only four of the eight shells are shown.*

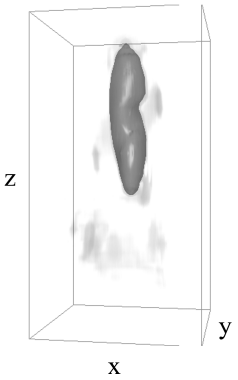


*Figure 2: 3D volume rendered from gradient-echo images from a homogeneous cylindrical phantom using the 3D selective technique.*

## Results and Discussion

Spatial localization produced by the 3D pulses is illustrated in Figure 2 for the phantom experiments. The target is well defined with a small amount of artifact (light grey) remaining in the suppression regions outside of the darker intended excitation volume. The results from the in vivo experiment are shown in Fig. 3. The target pattern was placed at isocenter in the transverse plane with the long axis of the corkscrew oriented with the anterior/posterior axis. The volume rendered from the 3D selective imaging experiment is shown with and without localizer overlay in Fig. 3a and 3b, respectively. The corresponding spectrum is shown in Fig. 3c. Fitting error estimates based on Cramer-Rao Lower Bound (CRLB) values are labeled for metabolites based on LCModel analysis. Only metabolites with CRLBs < 20% are given. Good spectral quality was realized as evident from the linewidths and ability to detect eight metabolites with significant accuracy including glutamate, glutamine, aspartate, and N-acetylaspartylglutamate.

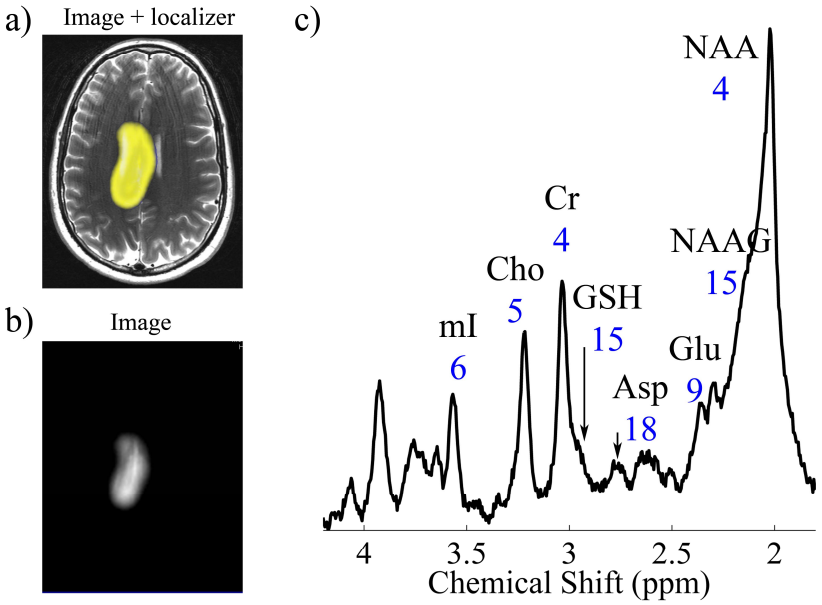


*Figure 3: In vivo 3D selective excitation data displaying: a) location of the target pattern (3D volume rendered from gradient echo images) in the transverse plane (yellow overlay) on a localizer image, b) 3D rendered volume only, and c) 128 average spectrum for the 3D method acquired with a 935 µs acquisition delay. Metabolites with CRLBS less than 20% are labelled at the most prominent peak locations (in the case of Cr, NAA and mI) in percent. Abbreviations used: mI – myo-inositol; Cho – choline; Cr – creatine; GSH – glutathione; Asp – aspartate; Glu – glutamate; NAAG – N-acetylaspartylglutamate; NAA – N-acetylaspartate.*

## Conclusion

The ability to select 3D arbitrary shapes in vivo at short echo times (or acquisition delays) offers many new applications of spectroscopy in healthy and diseased states for investigation of specific tissues. In this work, we have demonstrated excellent preliminary results which allow arbitrarily-shaped voxels in spectroscopy at an acquisition delay of 935 µs. The segmented technique provides broad excitation bandwidths allowing application of selective pulse schemes. Current technical investigations using this method include evaluation of excitation voxel leakage into the surrounding suppression region, and inclusion of parallel excitation to reduce the number of segments needed for full excitation (2). 3D shimming in vivo is crucially important to reduce off-resonance artifacts and further improvements may be obtained via inclusion of static field maps in the pulse calculation (3). Further planned experiments involve real-time planning of the 3D voxel to specific tissues in vivo in healthy volunteers.

## References

1. Qin Q, *et. al.* MRM 2007;58(1):19-26. 2. Snyder J, *et. al.* MRM 2011; doi: 10.1002/mrm.23018. 3. Grissom W, *et. al.* MRM 2006;56(3):620-629. 4. Provencher SW. MRM 1993;30:672-679.

**Acknowledgement:** This work is a part of the INUMAC project supported by the German Federal Ministry of Education and Research, grant #13N9208.